EXPERIMENTAL INVESTIGATION OF CREEP CRACK GROWTH FOR TWO HIGH TEMPERATURE ALLOYS

T. Hollstein*

The investigations show that the creep crack growth rate can be determined continuously with the single specimen partial unloading compliance technique and with the direct current potential drop technique with similar accuracy for temperatures up to 900°C and testing times up to nine months so far.

For compact and centre notched tension specimens the creep crack growth rates can be correlated to the loading parameter C*-Integral for the two materials X 6 Cr Ni 18 11 (similar to A 304 ss) and X 10 Ni Cr Al Ti 32 20 (Incoloy 800 H).

INTRODUCTION

Characterization of creep crack growth is important for the design of high temperature components and for a residual life time prediction of flawed components in service.

It is widely agreed that creep crack growth can be described independently of geometry by various fracture mechanics parameters like the stress intensity factor K [1,2], the C*-integral [2,3,4] and the C_t-parameter [5], provided that the specific conditions of the high stressed area in the crack tip zone are known, i.e. small scale creep with a creep zone which is small in comparison to the crack length and the other geometrical dimensions, steady state creep with a creep zone which penetrates the whole ligament of the component, and an intermediate state of transition creep, respectively. The limits of each parameter are discussed in detail by Riedel and Rice [6] and Saxena [5].

* Fraunhofer-Institut für Werkstoffmechanik, Wöhlerstrasse 11, D - 7800 Freiburg

This paper concentrates on experimental procedures for the determination of creep crack growth and on the correlation between creep crack growth and the fracture mechanics parameter C* for two materials.

MATERIALS AND SPECIMENS

The materials are a 18 % Cr 11 % Ni-stainless steel and a 32 % Ni 20 % Cr-alloy. The chemical composition and some mechanical properties are compiled in table 1.

The specimens used are compact (CT-) specimens with thicknesses B = 12.5 and 25 mm and widths W = 40 and 80 mm, respectively, and centre notched (CN-) tension specimens with B = 12.5 mm and W = 50 mm. They are shown in fig. 1.

Specimens with and without side grooves have been tested. The specimens were fatigue precracked according to the ASTM-rules to an a/W ratio of 0.53 for the CT-specimens and 0.3 for the CN-specimens. The final maximum fatigue load in most cases was smaller than the load applied during the creep test.

EXPERIMENTAL PROCEDURE

In most experiments the creep crack growth was determined using the direct current potential drop technique (DCPD). The current path through the specimen and the positions of the potential pick ups are indicated in fig. 1. A constant direct current is fed into the specimen in the plane of loading, and the potential drop φ is measured at two contact pins across the crack. φ changes when the specimen is loaded and especially when the crack grows. To exclude potential changes due to temperature or current variations φ is divided by a reference potential φ_{ref} which is measured periodically between the locations indicated in fig. 1, either on the specimen (1 in fig. 1) or across a reference piece of the same material (2 in fig. 1).

As an example the test data φ, φ_{ref}, $\varphi_N = \varphi/\varphi_{ref}$ and displacement V vs. time of a creep crack growth test with a CN-specimen loaded under a constant force of 46 kN at 600°C are shown in fig. 2. With the assumption that the correlation between the potential difference and crack growth is linear throughout the values under consideration crack growth rates can be determined with the initial and final values of φ or φ/φ_{ref}, and the amount of crack growth measured on the fracture surface after the test (see fig. 3).

For the example shown a fracture surface value of crack growth (sum of the extensions on both crack tips) $2\Delta a = 2.26$ mm was measured after the creep crack growth test. With that value and the potential differences taken from fig. 2 a crack growth rate

$da/dt = 4.3 \cdot 10^{-8}$ mm/s for $t \gtrsim 4 \cdot 10^6$ s is calculated. Depending on the choice of the initial values of φ or φ/φ_{ref} slightly different crack growth rates result. The initial value corresponding to onset of creep crack growth is often difficult to determine because effects of crack tip blunting, crack closure, change of conductivity with exposure time and corrosion may occur in the first stage of the test.

Using a normalized potential drop φ_N-measurement allows to eliminate the electrical conductivity. Then a unique value of $\Delta\varphi_N/\Delta a$ should exist for experiments with one specimen geometry and the same connection points for current and potential. Fig. 4 shows results for three different alloys tested at two temperatures under either constant force or constant rate of crack opening displacement measured at the load line. Using the mean value of $\Delta\varphi_N/\Delta a = 0.086$ mm^{-1} (see fig. 4) the crack growth rate in a similar experiment with an unknown material behaviour could be calculated.

Creep crack growth was determined in some specimens also using the partial unloading compliance technique (PUC). In this method the instantaneous crack length is calculated from measurements of the elastic compliance $C = \Delta V/\Delta F$ of the specimen and known functions of crack length $a = f$ (C,E, specimen geometry)(E=Young's modulus). The compliance is derived from small superimposed linear elastic unloadings ($\Delta F \approx 0.15$ F) as plotted for example in fig. 5. Figure 6 shows that both methods (DCPD and PUC) yield essentially the same creep crack growth. This justifies the assumption of a linear correlation between change of potential difference and crack growth that is used in the DCPD method.

The accuracy and the vanishing hystereses of the F-V-plot of the partial unloadings in fig. 5 are a consequence of the novel loading device [7] and measuring system for the crack opening displacement. Hardened on one side convex inserts (see fig. 7) allow for tilting on the flat bottom planes of the clevises if the loading pins are bent. In this way line load contact is maintained instead of point load. Thereby the risk of local plastic deformation of the clevis planes and restraint of necessary free rotation of the pins is minimized.

The crack opening displacement at the load line is measured outside the oven via quartz glass rods and linear variable differential transformer (LVDT). The LVDT's are hold by a system of springs which allow the transducer and the plunger to displace independently and nearly free of hysteresis and friction.

RESULTS

In fig. 8 results of creep crack growth tests are presented for the stainless steel X 6 Cr Ni 18 11 at 600°C. Plotted are creep crack growth rate versus C*-integral determined according to [3]

$$C^* = \frac{\eta F \cdot \dot{V}_c}{B(W-a)} \qquad (1)$$

η was chosen to be 2 for the CT-specimens and 1 for the CN-specimens. $\dot{V}_c$ is the displacement rate due to creep deformation only, excluding the displacement rate $\dot{V}_{crack}$ due to crack growth. Since $\dot{V}_{crack} \ll \dot{V}_{creep}$ for the ductile materials investigated here, the total displacement rate $\dot{V}$ was taken to calculate C*.

The results in fig. 8 can be described by a power law

$$\dot{a} = 9{,}03 \cdot 10^{-3} \cdot C^{*0.878} \qquad (2)$$

($\dot{a}$ in mm/s and C* in N/(mm·s)).

The results are independent of geometry, specimen size, loading condition and side grooves. In addition tests with a few load changes in particular towards lower stresses (see fig. 9) yield the same correlation. The transition time $t_1 \approx 2$ h (calculated according to Riedel and Rice [6]) indicates that steady-state creep conditions are present. The independence of geometrical factors and loading conditions shows the capability of the C*-integral model to describe crack growth under steady state conditions.

A comparison with mean values of creep crack growth resistance curves of different authors [3,8-11] for similar materials shows good agreement, see fig. 10.

Similar results with a power law correlation of $\dot{a}$ and C* were found for the alloy Incoloy 800 H at 800°C with a transition time $t_1 \approx 1$ h (see fig. 11). Tests with load changes for this alloy are reported in [12]; the results fit the scatterband of fig. 11.

CONCLUSIONS

The results presented here show that the creep crack growth rate can be determined continuously with the direct current potential drop and the partial unloading compliance technique; a similar accuracy is reached.

For each of the two alloys under investigation the creep crack growth rate is correlated with the C*-integral by a power law for increasing, constant and decreasing C*-tests. The correlations are independent of geometry, specimen size and loading conditions.

In consequence it should be possible to assess defects and to predict (residual) life times for flawed structures under steady state creep conditions on this basis.

REFERENCES

(1) Sadananda, K. and Shahinian, P., Metallurgical Transactions, Vol. 8A, 1977, pp. 439-449

(2) Riedel, H. and Wagner, W., "Creep Crack Growth in Nimonic 80 A and in a 1 Cr-1/2 Mo Steel", Proceedings of the 6th Int. Conf. on Fracture. Edited by S.R. Valluri, J.F. Knott, P. Rama Rao and D.M.R. Taplin, Pergamon Press, Oxford, 1984

(3) Koterazawa, R. and Mori, T., Transactions of the ASME, Journal of Engineering Materials and Technology, Vol. 99, 1977, pp. 298-305

(4) Nikbin, K.M., Webster, G.A. and Turner, C.E., "Relevance of Nonlinear Fracture Mechanics to Creep Cracking", Cracks and Fracture, ASTM STP 601, American Society for Testing and Materials, 1976, pp. 47-62

(5) Saxena, A., "Creep Crack Growth under Non Steady - State Conditions", Scientific Paper 84-107-EVFLA-P2, Westinghouse, Pittsburgh, PA, U.S.A., 1984

(6) Riedel, H. and Rice, J.R., "Tensile Cracks in Creeping Solids", Fracture Mechanics: Twelfth Conference, ASTM STP 700, American Society for Testing and Materials, 1980, pp. 112-130

(7) Voss, B. and Mayville, R.A., "The Use of the Partial Unloading Compliance Method for the Determination of J_I-R Curves and J_{Ic}, "Elastic-Plastic Fracture Test Methods: The User's Experience, ASTM STP 856, Eds. E.T. Wessel and F.J. Loss, American Society for Testing and Materials, 1985, pp. 117-130

(8) Saxena, A., "Evaluation of C* for the Characterization of Creep-Crack-Growth Behavior in 304 Stainless Steel", Fracture Mechanics: Twelfth Conference, ASTM STP 700, American Society for Testing and Materials, 1980, pp. 131-151

(9) Musicco, G.G., Boerman, D.J. and Riatti, G., "Creep Crack Growth Characterization of Austenitic Stainless Steel", Advances in Fracture Research, Proceedings of 5th Int. Conf. on Fracture (ICF), Ed. D. Francois, Pergamon Press, Oxford, 1981, pp. 1323-1331

(10) Krompholz, K., Huthmann, H., Grosser, E.D. and Pierick, J.B., Engineering Fracture Mechanics 16, 1982, pp. 809-819

(11) Shih, T.T., "A Simplified Test Method for Determining the Low Rate Creep Crack Growth Data", Fracture Mechanics: Fourteenth Symposium - Volume II: Testing and Applications, ASTM STP 791, Eds. J.C. Lewis and G. Sines, American Society for Testing and Materials, 1983, pp. II/232-II/247

(12) Hollstein, T. and Blauel, J.G., "Fracture Mechanics Characterization of Crack Growth under Creep-Fatigue Conditions", IWM-Report Z 1/85, Freiburg, 1985

ACKNOWLEDGEMENT: The author is grateful to the Deutsche Forschungsgemeinschaft for the financial support to pursue this investigation.

TABLE 1 - Chemical composition and mechanical properties at room temperature

	weight - %						
Material	C	Si	Mn	P	S	Cr	Ni
X 6 Cr Ni 18 11 (Similar to A 304 ss)	.054	.50	1.74	.024	.009	18.2	10.7
X 10 Ni Cr Al Ti 32 20 (Incoloy 800 H)	.070	.46	.68	.020	.004	20.26	31.11

	weight - %					
Material	Mo	N	B	Al	Ti	Ti+Nb+Ta
X 6 Cr Ni 18 11	.09	.053	.0001			.03
X 10 Ni Cr Al Ti 32 20				.34	.31	

Material	$R_{po.2}$ [MPa]	R_{p1} [MPa]	R_m [MPa]	A [%]	Z [%]
X 6 Cr Ni 18 11	235	267	563	38	75
X 10 Ni Cr Al Ti 32 20	252	291	575	46	74

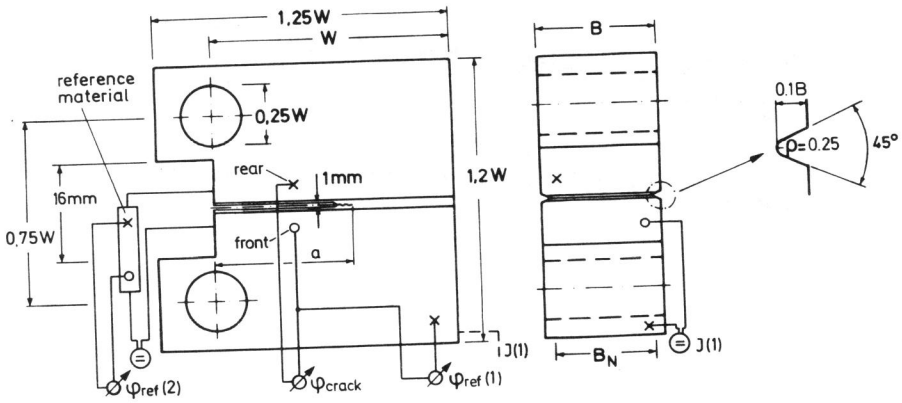

Figure 1a Compact (CT-) specimen

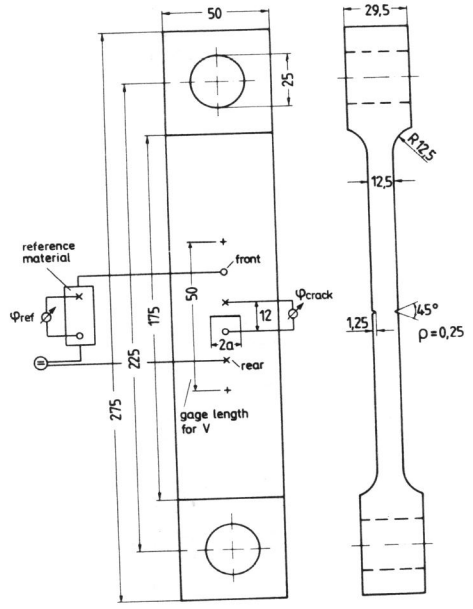

Figure 1b Centre notched (CN-) specimen

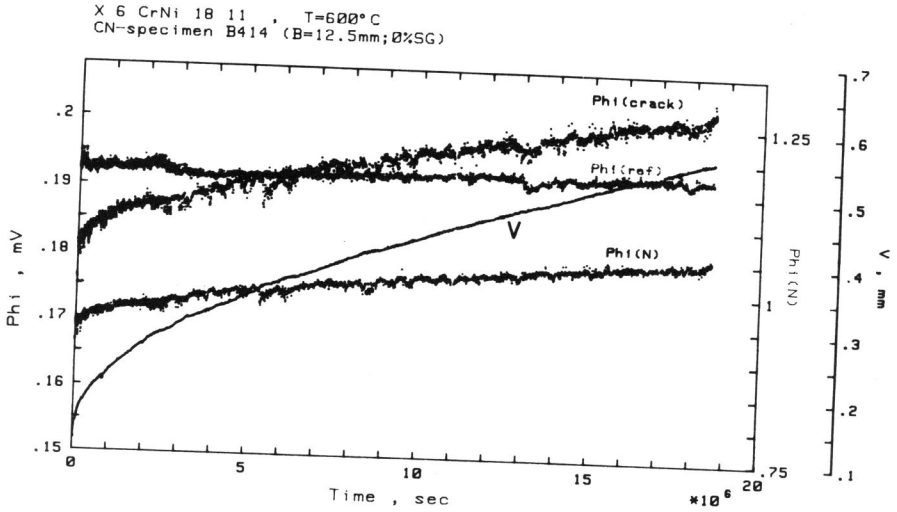

Figure 2 Primary data of a creep crack growth test with a centre notched tension specimen at 600°C (F = 46 kN)

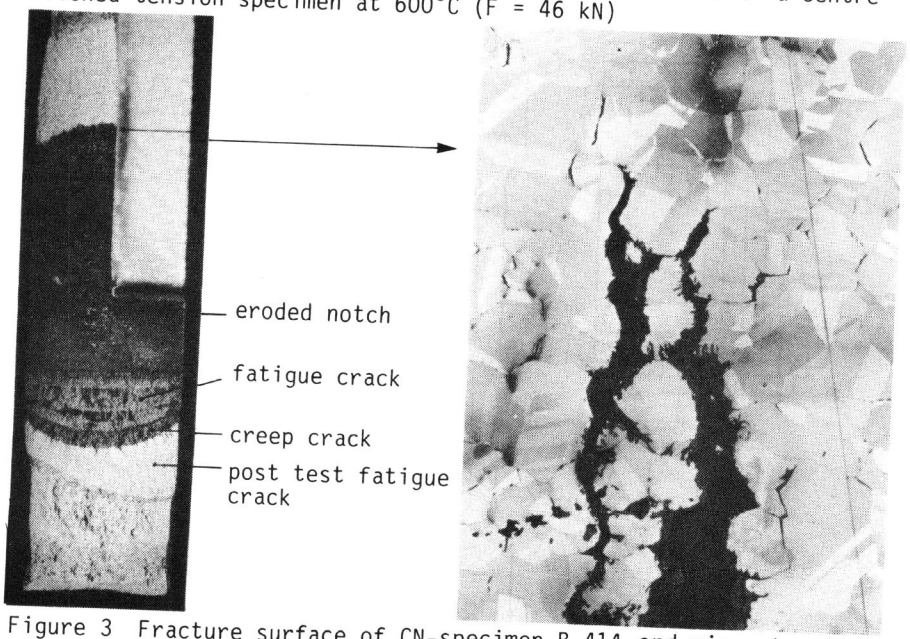

Figure 3 Fracture surface of CN-specimen B 414 and microstructure of the crack tip area

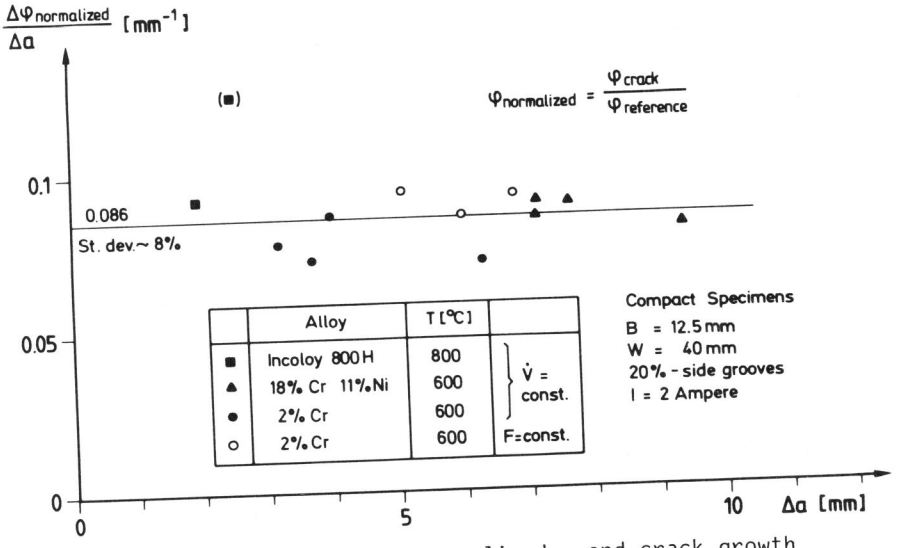

Figure 4 Correlation between normalized φ and crack growth (connection points 1 and 2 in fig. 1)

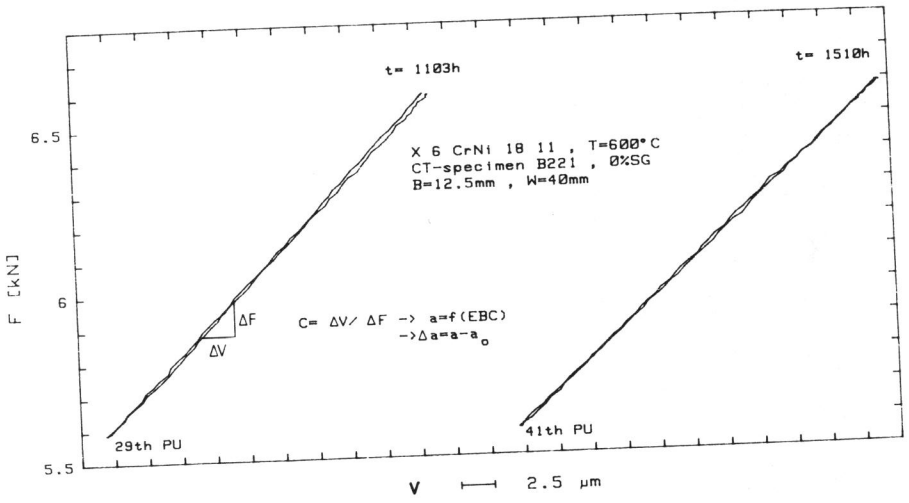

Figure 5 Details of two partial unloadings

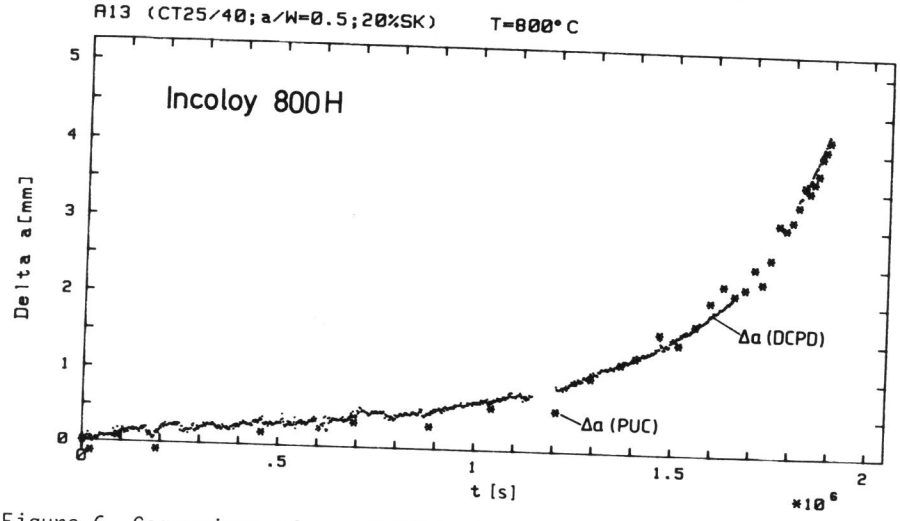

Figure 6 Comparison of Δa (DCPD) with Δa (PUC)

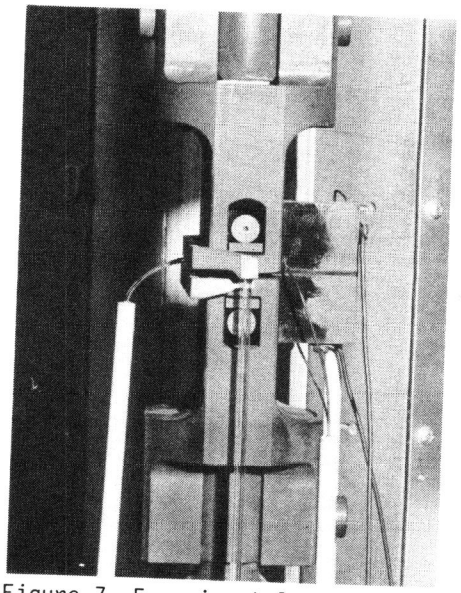

Figure 7 Experimental arrangement

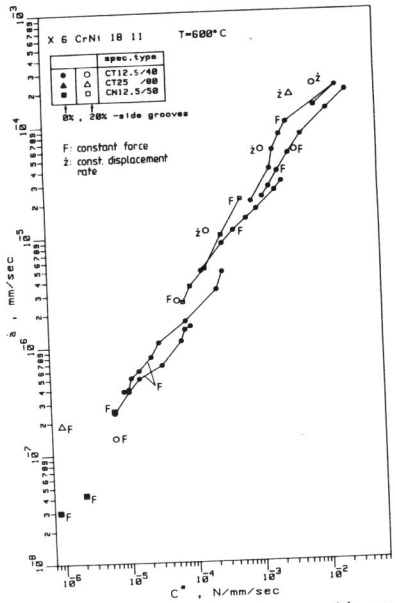

Figure 8 Creep crack growth rate versus C*-integral

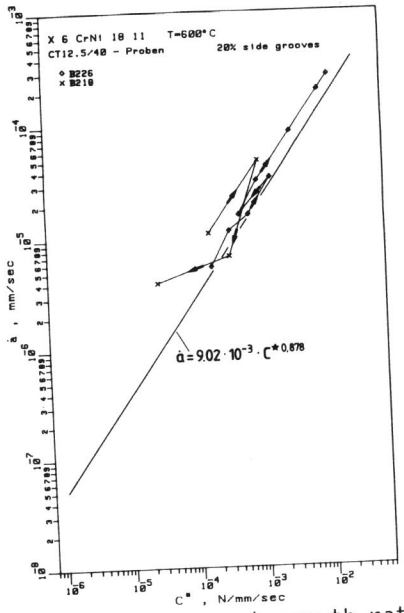

Figure 9 Creep crack growth rate versus C*-integral for tests with load changes

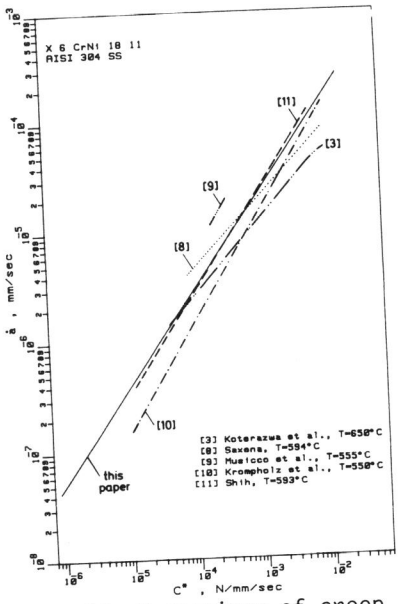

Figure 10 Comparison of creep crack growth curves of different authors

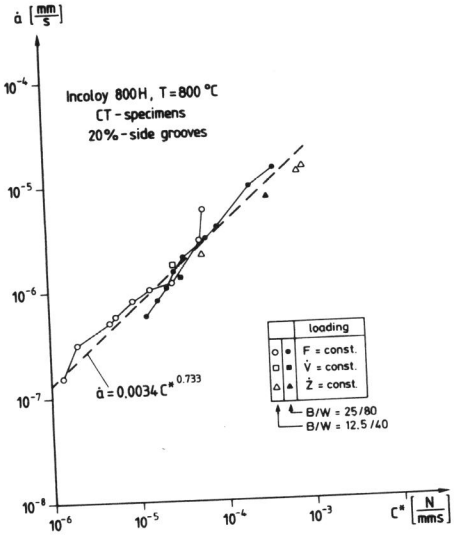

Figure 11 Crack growth rate resistance curves for the alloy Incoloy 800 H